A Common Electromagnetic Framework for Carbon Nanotubes and Solid Nanowires—Spatially Dispersive Conductivity, Generalized Ohm's Law, Distributed Impedance, and Transmission Line Model

George W. Hanson, *Fellow, IEEE*

***Abstract*—General equations are presented for the spatially dispersive conductivity, distributed impedance, Ohm's law relation, and transmission line model of both carbon nanotubes (CNTs) and solid material nanowires. It is shown that spatial dispersion results in an intrinsic (material-dependent) transmission-line capacitance. Spatial dispersion is numerically unimportant in metal nanowires, but leads to a shift in propagation constant of a few percent for CNTs and semiconducting nanowires. Theoretically, spatial dispersion is important for both nanowires and nanotubes, and is necessary to preserve the inductance–capacitance–velocity relation $L_k C_{\rm dos} = v_F^2$, where L_k is kinetic inductance, $C_{\rm dos}$ is intrinsic capacitance, and v_F is electron Fermi velocity. It is shown that in order to obtain the correct intrinsic capacitance, it is necessary to use a charge-conserving form of the relaxation-time approximation to Boltzmann's equation. Numerical results for the propagation constant of various nanowires and CNTs are presented. The general formulation developed here allows one to compute, and directly compare and contrast, properties of CNTs and solid nanowires.**

***Index Terms*—Carbon nanotubes (CNTs), multiconductor transmission lines (MTLs), nanotechnology.**

I. Introduction

CARBON nanotubes and metal nanowires have been recently considered as interconnects for future electronic systems [1]–[12]. Various configurations are possible, such as single-wall nanotubes, multiwall nanotubes, and bundles of various nanotube types. Although single-wall nanotubes typically have radius values less than 1–2 nm, control over effective radius can be achieved using multiwall tubes or tube bundles. These systems have been predicted to outperform nanowires in some cases [7]–[12], particularly for relatively large bundles of small-radius single-wall tubes. However, lacking sufficient control over geometry, nanowires may perform better, and can also come as single or bundled structures. Thus, at this stage, both carbon nanotubes (CNTs) and solid nanowires are of considerable interest, from both a theoretical and practical standpoint.

Manuscript received April 03, 2010; revised August 12, 2010; accepted September 22, 2010. Date of publication December 03, 2010; date of current version January 12, 2011.

The author is with the Department of Electrical Engineering, University of Wisconsin–Milwaukee, Milwaukee, WI 53211 USA (e-mail: george@uwm.edu).

Color versions of one or more of the figures in this paper are available online at http://ieeexplore.ieee.org.

Digital Object Identifier 10.1109/TMTT.2010.2090693

In this paper, we consider a common electromagnetic model for CNTs and solid nanowires. We will assume that these structures are formed by electrically thin ($a \ll \lambda$, where a is radius and λ is wavelength) conducting materials with length much longer than radius, oriented parallel to the z axis. Accordingly, we neglect any transverse current and consider only longitudinal current. The main assumption is that the material response is due to intraband conduction electrons such that Boltzmann's transport equation provides an appropriate description of the electromagnetic field–material interaction. The analysis is applicable below the range of electron interband transitions, which occurs at tens of THz for CNTs and hundreds of THz for metals, and for CNTs assumes operation near the Fermi point $\mu = 0$.

It is shown that the usual relaxation time approximation (RTA) of Boltzmann's equation is not adequate to account for spatial dispersion, which is intimately connected with diffusion and intrinsic capacitance. A modified RTA, which preserves charge continuity, is shown to lead to the correct result that preserves the inductance–capacitance–velocity relation $L_k C_{\rm dos} = v_F^2$. A general expression for the spatially dispersive conductivity is derived, which leads to a common form for the distributed impedance of solid nanowires and CNTs. A general transmission line model is developed, where spatial dispersion is shown to be associated with intrinsic capacitance $C_{\rm dos}$ (sometimes called a finite density-of-states capacitance or, more often, a quantum capacitance). The formulation arises purely from Boltzmann's equation and Maxwell's equations, rather than from a transmission line approach that starts with a given configuration of circuit elements. It will be shown that spatial dispersion in metal nanowires is numerically negligible, but leads to effects on the order of a few percent for CNTs and semiconducting nanowires. The same methods also carry over to the analysis of graphene, but this is not included in this paper due to limited space.

The Boltzmann model provides a semiclassical treatment of electron dynamics, and in a fully numerical procedure the Boltzmann/Maxwell system can be solved simultaneously. Here it is solved in the limit of small perturbations from equilibrium, leading to the closed-form result (1). As an alternative to the Boltzmann/Maxwell model, a Schrödinger/Maxwell model is developed in [13]–[15]. Schrödinger's equation is a fully quantum model for electron dynamics. However, it should be noted that the exact many-electron Schrödinger equation (i.e., using the exact potential and the N-particle

wavefunction including exchange correlations) is not actually solved since this is practically impossible, but rather, an envelope function Schrödinger equation (the typical effective mass model) is solved. This approximation has a similar spirt to the fact that Boltzmann's equation does not consider the movement of individual electrons, but uses statistical mechanics to formulate an equation for the electron distribution function. Therefore, both Boltzmann's and Schrödinger's equation (as used) approximate electron dynamics, even if used in a fully numerical simultaneous solution with Maxwell's equations. A simultaneous numerical solution should provide more accurate results for higher electron energies, beyond the validity of the perturbation approach. Moreover, the method of [13]–[15] allows for boundary conditions on both electrons and photons, whereas the closed-form Boltzmann model used here assumes the structure is infinite for electrons, allowing the definition of material conductivity (in a numerical solution of Boltzmann's equations boundary conditions on the electron distribution function could be applied). Both the Schrödinger/Maxwell and Boltzmann/Maxwell models should provide similar results for frequencies of interest in this paper.

The main new results of the paper are presented in the following sections with most of the derivations appearing in the Appendix. Throughout this paper, SI units are used, and the (suppressed) time dependence is $e^{j\omega t}$.

II. General Results for Spatially Dispersive Conductivity, Current-Field Relationship, and Generalized Impedance

For the considered class of cylindrical structures the spatially dispersive conductivity $\sigma(q,\omega)$ has the general form

$$\sigma(q,\omega)=\frac{j2e^2}{(\omega-j\tau^{-1})}\left(I(q,\omega)^{-1}-\frac{j2\beta\alpha q^2\tau^{-1}}{\omega(\omega-j\tau^{-1})^2}\right)^{-1} \quad (1)$$

where

$$I(q,\omega)=\int\frac{v_z^2}{1-\left(\frac{qv_z}{(\omega-j\tau^{-1})}\right)^2}\frac{\partial f_0}{\partial\varepsilon}d\mathbf{k}. \quad (2)$$

In the above expressions, q is the spatial wavenumber, ω is radian frequency, τ is a phenomenological electron relaxation time, v_z is the longitudinal electron velocity, f_0 is the equilibrium Fermi–Dirac distribution, $-e$ is the electron charge, ε is electron energy, $\mathbf{k}$ is electron quasi-momentum, β is a geometrical constant ($\beta=2\pi a$ and 1 for CNTs and solid nanowires, respectively), and α is a material-dependent quantity defined later. The second term in (1), which is absent in the usual RTA solution of Boltzmann's equation, provides an important contribution, as described later.

The distributed impedance (Ω/m) of these structures can be defined as $z=1/2\pi a\sigma(q,\omega)$ for CNTs and $z=1/\pi a^2\sigma(q,\omega)$ for solid nanowires. These lead to the general form

$$z=R+j\omega L_k+\frac{q^2}{j\omega C_{\rm dos}}\varsigma(\omega) \quad (3)$$

where per-unit-length quantities R, L_k, and $C_{\rm dos}$ are the resistance, kinetic inductance, and intrinsic (density of states or quantum) capacitance, respectively, of the material, and where $\varsigma(\omega)$ is a material-specific parameter of order unity defined later ($\varsigma=1$ for CNTs and $\varsigma=O(1)$ for solid nanowires). In [3], the concepts of kinetic inductance and quantum capacitance have been introduced for a general nanowire.

Both CNTs and solid nanowires satisfy a generalized Ohm's law

$$(1-\xi q^2)J(q,\omega)=\sigma(\omega)E(q,\omega) \quad (4)$$

where $\sigma(\omega)$ is the usual local Drude conductivity, and ξ is a spatial dispersion parameter ($|\xi|q\ll 1$). For CNTs, this relation was first derived in [16], and here we show that it is also applicable to solid nanowires, and that the spatial dispersion parameter ξ requires special treatment. The generalized Ohm's law (4) is equivalent to a 1-D drift-diffusion model [17] (see also [27] where a fluid model accommodating diffusion is presented),

$$J_z(z,\omega)=\sigma(\omega)E_z(z,\omega)+\frac{D}{j\omega}\frac{d^2J_z(z,\omega)}{dz^2} \quad (5)$$

where the diffusion constant is $D=-j\omega\xi$. Thus, one can solve either (4) in the transform domain, or (5) in the space domain.

For solid nanowires, the term $(1-\xi q^2)$ is actually $(1-\xi_2q^2-\xi_4q^4+\cdots)$, but the higher order terms are negligible, and for CNTs, the higher order terms are identically zero. Thus,

$$\sigma(q,\omega)=\sigma(\omega)(1-\xi q^2)^{-1}\simeq\sigma(\omega)(1+\xi q^2) \quad (6)$$

is equivalent to (1) for CNTs, and provides an excellent approximation to (1) for solid nanowires.

The generalized Ohm's law (4) leads to the general integral equation

$$\left(k^2+\frac{\partial^2}{\partial z^2}\right)\int K(z-z')I(z')dz' =\frac{j2\omega\varepsilon}{\nu a\sigma(\omega)}\left(1+\xi\frac{\partial^2}{\partial z^2}\right)I(z)-j2\pi\omega\varepsilon E_z^i(z) \quad (7)$$

where $K(z-z')$ is the usual kernel ($K(z-z')=\int_{-\pi}^{\pi}d\phi'(e^{-jkR})/(4\pi R)$) and $\nu=2$ for CNTs and $\nu=a$ for solid cylinders.

The role of spatial dispersion can be appreciated by considering an infinitely long structure. $J_z(q,\omega)=\sigma(q,\omega)E_z(q,\omega)$ then leads to the space-domain current in the usual nonlocal form

$$J_z(z,\omega)=\int_{-\infty}^{\infty}\sigma(z-z',\omega)E_z(z',\omega)dz' \quad (8)$$

where $\sigma(z,\omega)$ is the inverse Fourier transform of $\sigma(q,\omega)$. The conductivity can be evaluated using complex-plane analysis, leading to

$$\sigma(z,\omega)=\frac{1}{2}\gamma\sigma(\omega)e^{-\gamma|z|}. \quad (9)$$

where $\gamma=j\xi^{-1/2}$. The range of nonlocality is the range of distance $|z-z'|$ for which $\sigma(z-z',\omega)$ is appreciably different from zero. Since we can represent the delta function as $\delta(z)=\lim_{\beta\to0}e^{-|z|/\beta}/2\beta=\lim_{\gamma\to\infty}\alpha e^{-\gamma|z|}/2$ ($\gamma=1/\beta$), we have

$$\lim_{\gamma=\to\infty}\sigma(z,\omega)=\sigma(\omega)\delta(z). \quad (10)$$

Thus, we recover the local limit as $\gamma = j\xi^{-1/2} \to \infty$, which, as shown later, corresponds to $\tau \to 0$. Therefore, a local conductivity is obtained in the limit of vanishing electron mean-free path.

III. Specific Expressions for CNTs and Solid Nanowires, and Numerical Comparisons

In this section, we present some specific results for CNTs and solid nanowires (these are derived in the Appendix). For nanowires, the conductivity (1) and the spatial dispersion parameter ξ are

$$\sigma^{\text{solid}}(q,\omega) = \sigma_0 \frac{3j(\omega - j\tau^{-1})}{v_F^2 q^2 \tau} \times \left\{ \left(1 + \frac{\omega - j\tau^{-1}}{2v_F q} \times \ln\left(\frac{\omega - j\tau^{-1} - v_F q}{\omega - j\tau^{-1} + v_F q} \right) \right)^{-1} - \frac{j}{\omega\tau} \right\}^{-1} \tag{11}$$

$$\simeq \sigma(\omega)(1 - \xi^{\text{solid}} q^2)^{-1} \tag{12}$$

$$\xi^{\text{solid}} = \frac{j v_F^2 \tau}{\omega(1 + j\omega\tau)} \varsigma \tag{13}$$

where $\sigma(\omega) = \sigma_0/(1 + j\omega\tau)$ (S/m) is the usual Drude conductivity ($\sigma_0 = e^2\tau n/m$ is the dc conductivity where n is the electron density, m^{-3}, [18]) and

$$\varsigma = \frac{1}{3} \frac{1 + \frac{9}{5} j\omega\tau}{1 + j\omega\tau} \tag{14}$$

is a parameter of order unity ($1/3 \le \varsigma \le 3/5$).

The distributed impedance (Ω/m) is

$$z_{\text{solid}} = \frac{1}{\pi a^2 \sigma(q,\omega)} = R^{\text{solid}} + j\omega L_k^{\text{solid}} + \frac{q^2}{j\omega C_{\text{dos}}^{\text{solid}}} \varsigma \tag{15}$$

where

$$R^{\text{solid}} = \frac{1}{\pi a^2 \sigma_0} \quad L_k^{\text{solid}} = \tau R^{\text{solid}} \tag{16}$$

$$C_{\text{dos}}^{\text{solid}} = \pi a^2 \frac{me^2}{(3\hbar^3\pi^2)^{2/3}} n^{1/3}. \tag{17}$$

We have included the factor πa^2 in the definition of C_{dos} to be consistent with R and L_k (so that $L_k^{\text{solid}} C_{\text{dos}}^{\text{solid}} = m^2/(3\hbar^3\pi^2 n)^{2/3} = 1/v_F^2$, where v_F is the Fermi velocity), and to obtain a capacitance with the units of F/m, in order to facilitate comparison with CNTs.

For small-radius single-wall CNTs,

$$\sigma^{\text{cnt}}(q,\omega) = \frac{-j2e^2 v_F}{\hbar\pi^2 a(\omega - i\tau^{-1})} \left(1 - \frac{q^2 v_F^2}{\omega(\omega - i\tau^{-1})} \right)^{-1} \tag{18}$$

$$= \sigma(\omega)(1 - \xi^{\text{cnt}} q^2)^{-1} \tag{19}$$

$$\xi^{\text{cnt}} = \frac{j v_F^2 \tau}{\omega(1 + j\omega\tau)} \tag{20}$$

where $\sigma(\omega) = 2e^2 v_F \tau/\hbar\pi^2 a(1 + j\omega\tau)$ (S) is the local Drude conductivity. Note that ξ^{cnt} and ξ^{solid} have the same form, except for the near-unity factor ς.

The distributed impedance (Ω/m) is

$$z_{cn}(q,\omega) = \frac{1}{2\pi a \sigma(q,\omega)} = R^{\text{cnt}} + j\omega L_k^{\text{cnt}} + \frac{q^2}{j\omega C_{\text{dos}}^{\text{cnt}}} \tag{21}$$

where

$$R^{\text{cnt}} = \frac{h}{4e^2} \frac{1}{2v_F\tau} = \frac{R_0}{4v_F\tau} \tag{22}$$

$$L_k^{\text{cnt}} = \tau R = \frac{1}{4} \frac{h}{2e^2 v_F} = \frac{R_0}{4v_F} \tag{23}$$

$$C_{\text{dos}}^{\text{cnt}} = \frac{8e^2}{h v_F} = \frac{4}{R_0 v_F} \tag{24}$$

where $R_0 = h/2e^2$ is the resistance quantum. We have $L_k^{\text{cnt}} C_{\text{dos}}^{\text{cnt}} = 1/v_F^2$, where v_F is the electron Fermi velocity in the nanotube, as expected. The values of L_k^{cnt} and $C_{\text{dos}}^{\text{cnt}}$ agree with independently derived expressions [1] (see also [19] and [20]). The expression for the resistance R^{cnt} agrees with that obtained in [3], and provides values that are in reasonable agreement with experiment [2]. Note that these values are independent of nanotube radius. This holds as long as the nanotube radius is sufficiently small so that only two electron channels exist (which typically holds for single-wall nanotubes).

It is interesting to numerically compare these parameters for CNTs and nanowires. The parameters R, L_k, and C_{dos} are frequency independent, and for the frequency-dependent parameter ξ, we assume $\omega = 10$ GHz. For CNTs, we use the typical values $v_F^{\text{cnt}} = 9.71 \times 10^5$ m/s and $\tau^{\text{cnt}} = 5 \times 10^{-13}$ s, such that

$$R^{\text{cnt}} = 6.65\ \text{k}\Omega/\mu\text{m} \tag{25}$$

$$L_k^{\text{cnt}} = 3.32\ \text{nH}/\mu\text{m} \tag{26}$$

$$C_{\text{dos}}^{\text{cnt}} = 320\ \text{aF}/\mu\text{m} \tag{27}$$

$$\xi^{\text{cnt}} = 2.36 \times 10^{-13} + j4.71 \times 10^{-11}\ \text{m}^2 \tag{28}$$

$$\gamma^{\text{cnt}} = \frac{j}{\sqrt{\xi^{\text{cnt}}}} = 0.103 + j0.103/\mu\text{m}. \tag{29}$$

For gold nanowires (other typical metals of interest have similar electrical properties) with $n^{\text{au}} \sim 5.90 \times 10^{28}\ \text{m}^{-3}$, $\tau^{\text{au}} = 2.74 \times 10^{-14}$ s, $\sigma_0^{\text{au}} = 4.55 \times 10^7$ S/m, and $v_F^{\text{au}} = 1.39 \times 10^6$ m/s (here we are using the bulk material properties—electron surface and grain-boundary scattering may change these values for nanowires, usually by less than an order of magnitude [21], [22]), we obtain

$$R^{\text{au}}|_{a=50\ \text{nm}} = 0.0028\ \text{k}\Omega/\mu\text{m} \tag{30}$$

$$L_k^{\text{au}}|_{a=50\ \text{nm}} = 0.0767\ \text{pH}/\mu\text{m} \tag{31}$$

$$R^{\text{au}}|_{a=10\ \text{nm}} = 0.070\ \text{k}\Omega/\mu\text{m} \tag{32}$$

$$L_k^{\text{au}}|_{a=10\ \text{nm}} = 1.92\ \text{pH}/\mu\text{m} \tag{33}$$

$$C_{\text{dos}}^{\text{au}}|_{a=50\ \text{nm}} = 6.72\ \text{pF}/\mu\text{m} \tag{34}$$

$$C_{\text{dos}}^{\text{au}}|_{a=10\ \text{nm}} = 0.269\ \text{pF}/\mu\text{m} \tag{35}$$

$$\xi^{\text{au}} = 9.70 \times 10^{-17} + j1.77 \times 10^{-12}\ \text{m}^2 \tag{36}$$

$$\gamma^{\text{au}} = \frac{j}{\sqrt{\xi^{\text{au}}}} = 0.531 + j0.531/\mu\text{m}. \tag{37}$$

It can be seen that the spatial dispersion parameters $\xi^{\rm au}$ and $\xi^{\rm cnt}$ are somewhat similar, and only differ by one order of magnitude. Accordingly, from (9), it can be seen that the range of nonlocality is governed by $\mathrm{Re}(\gamma)$, and $\gamma^{\rm cnt}$ is similar to $\gamma^{\rm au}$. This can be understood since, aside from the factor ς, which is order 1, $\xi^{\rm solid}$ and $\xi^{\rm cnt}$ have the same functional form. Since v_F is similar for CNTs and metals, then the main numerical difference comes from the value of τ in the expression for ξ. These differ by not quite an order of magnitude for the values chosen here (at most there is likely to be only one to two orders of magnitude difference). Thus, single-wall CNTs are, intrinsically, only slightly more nonlocal than metals, and the difference arises from the electron relaxation time. However, as shown below, there is a strong geometric influence that renders spatial dispersion less important in nanowires made from good conductors (which cannot be fabricated at the 1–2-nm dimensions typical of single-wall nanotubes).

As shown in the Appendix, in the development of the distributed impedance, the circuit manifestation of spatial dispersion is the intrinsic density-of-states capacitance (if $\xi = 0$, the capacitance term $C_{\rm dos}$ is absent). For a solid nanowire, other than the factor ς that is of order 1, $C_{\rm dos}$ contains a factor πa^2 and is radius dependent. Assuming $a = 10$ nm as the smallest reasonable metal radius, $C_{\rm dos}^{\rm au} = 2.69\times 10^5$ aF/μm, whereas for a CNT $C_{\rm dos} = 320$ aF/μm. Thus, the intrinsic capacitance is at least three orders of magnitude larger for a metal nanowire, and grows as a^2. Therefore, the effective intrinsic capacitive reactance is much smaller for a metal nanowire than for a nanotube, and can typically be neglected in all but the smallest nanowires. Similarly, the kinetic inductance involves a factor $1/\pi a^2$, and at $a = 10$ nm is at least three orders of magnitude smaller for the metal nanowire than for a CNT. The resistance is approximately two orders of magnitude smaller for a metal nanowire than for a CNT, and quickly decreases as radius increases ($R \sim 1/a^2$).

Since the intrinsic capacitive reactance in metal nanowires can typically be neglected, spatial dispersion in these structures can typically be neglected in numerical computations. However, from (17), it is clear that this is not be the case for a material having lower electron density (typically, lower conductivity). For example, consider a degenerately doped semiconductor having $n = 10^{23}$ m^{-3}. At this degree of doping, we can treat the material as a metal-like plasma, although accounting for effective mass. For GaAs with this doping level at room temperature, $\sigma_0 \sim 10^4$ S/m, $\tau \sim 2\times 10^{-13}$ s [23], and $v_F \sim 2.6\times 10^5$ m/s, leading to ($a = 10$ nm) $C_{\rm dos}^{\rm GaAs} = 227$ aF/μm, which is similar to that for the CNT. Thus, the capacitive reactance and spatial dispersion in a degenerately doped semiconductor are numerically important. The same would be true of a simple lower conductivity metal.

For a gold nanowire having $a = 10$ nm at $\omega = 10^{10}$ Hz,

$$z_m^{\rm au} = R^{\rm au} + j\omega L_k^{\rm au} + \frac{q^2}{j\omega C_{\rm dos}^{\rm au}}\varsigma \tag{38}$$

$$= 7.0\times 10^7 + j(19200 - 1.24\times 10^{-4}q^2) \tag{39}$$

$$= 7.0\times 10^7 + j(1.92 - 0.0014)\times 10^4 \tag{40}$$

where the last line comes from assuming $q = 10k_0$ as a reasonable value. It can be seen that the capacitive reactance is clearly negligible, and that the kinetic inductive reactance is three orders of magnitude smaller than the resistance. For a CNT,

$$z_{cn}(q,\omega) = R^{\rm cnt} + j\omega L_k^{\rm cnt} + \frac{q^2}{j\omega C_{\rm dos}^{\rm cnt}} \tag{41}$$

$$= 3.32\times 10^9 + j(3.32\times 10^7 - 0.3125q^2) \tag{42}$$

$$= 3.32\times 10^9 + j(3.32 - 0.0035)\times 10^7 \tag{43}$$

where we again assume $q = 10k_0$ in the last line. Clearly, in both cases, the impedance is dominated by the resistance, although for the CNT, the kinetic inductive reactance is quite important.

Although quantitatively incorrect, it is worthwhile to consider a fictitious metal conductor having $a = 1$ nm. Although this radius is not realistic, it allows one to reduce geometrical effects and more directly compare nanotubes and metal nanowires (if nanowires could have similar radius values). We obtain

$$R|_{a=1\text{ nm}} = 7.0\ \text{k}\Omega/\mu\text{m} \tag{44}$$

$$L_k|_{a=1\text{nm}} = 0.19\ \text{nH}/\mu\text{m} \tag{45}$$

$$C_{\rm dos}|_{a=1\text{ nm}} = 2686.9\ \text{aF}/\mu\text{m} \tag{46}$$

and

$$z_m = R + j\omega L_k + \frac{q^2}{j\omega C_{\rm dos}}\left(\frac{1}{3}\frac{1+\frac{9}{5}j\omega\tau}{1+j\omega\tau}\right) \tag{47}$$

$$= 7\times 10^9 + j(1.92\times 10^6 - 1.2407\times 10^{-2}q^2) \tag{48}$$

$$= 7\times 10^9 + j(1.92 - 0.0014)\times 10^6 \tag{49}$$

for $q = 10k_0$. The resistance is similar to the nanotube value, whereas the reactance is one order of magnitude smaller. It can be seen that the performance of these two structures would be similar. Note that if $\tau^{\rm cnt}$ were larger, which is possible, than the resistance of the nanotube would decrease. The value $\tau^{\rm cnt} = 5\times 10^{-13}$ s is consistent with a mean-free path of around 500 nm, whereas $\tau^{\rm cnt} = 10^{-12}$ s leads to a mean-free path of almost 1 μm, which is also a reasonable value and which would halve the resistance.

IV. Transmission Line Analysis

In this section, we obtain the modal properties and transmission line parameters for electromagnetically coupled CNTs or nanowires in a homogeneous dielectric ε. We assume that the nanotubes or wires are infinity long, oriented parallel to the z-axis, and that the radius of the nth tube is a_n (and, hence, has conductivity σ_n). The formulation proceeds from Maxwell equations and the Boltzmann equation conductivity, and we do not assume a certain transmission line configuration.

We first consider two electromagnetically coupled conductors (we assume that the conductors are not electronically coupled; i.e., there is no wavefunction overlap or quantum tunneling). Assume that one conductor carries current I_1, has radius a_1, and is centered at $\rho = 0$, and the other conductor carries current I_2, has radius a_2, and is centered at $\rho = b$, as shown in Fig. 1.

The total field E_z for the first conductor is the field due to current on the first conductor (I_1), plus the field due to current

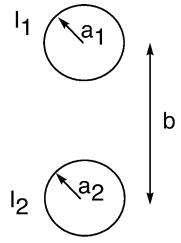

Fig. 1. Two electromagnetically coupled CNTs or solid nanowires.

on the second conductor (I_2), plus any incident field. For the second conductor, we have a similar situation, and thus, from (7), we obtain a set of two coupled integral equations

$$\left(1+\xi_1\frac{\partial^2}{\partial z^2}\right)\frac{I_1(z)}{\nu_1\pi a_1\sigma_1} \tag{50}$$

$$=\frac{1}{j4\pi\omega\varepsilon}\left(k^2+\frac{\partial^2}{\partial z^2}\right)(I_{11}+I_{12})+E^i_{z,1} \tag{51}$$

$$\left(1+\xi_2\frac{\partial^2}{\partial z^2}\right)\frac{I_2(z)}{\nu_2\pi a_2\sigma_2}$$

$$=\frac{1}{j4\pi\omega\varepsilon}\left(k^2+\frac{\partial^2}{\partial z^2}\right)(I_{21}+I_{22})+E^i_{z,2} \tag{52}$$

for all $-\pi\le\phi\le\pi, -\infty<z<\infty$, where $E^i_{z,n}$ is the incident field on conductor n and

$$I_{\alpha\beta}=\int_{-\infty}^{\infty}\int_{-\pi}^{\pi}\frac{e^{-jkR_{\alpha\beta}}}{R_{\alpha\beta}}\frac{I_\beta(z')}{2\pi}d\phi' dz'. \tag{53}$$

Note that we can have a metal nanowire coupled to a CNT.

For both source points $(\mathbf{r}')$ and observation points $(\mathbf{r})$ on the first conductor, or both on the second conductor, $\rho=\rho'=a$ and $R_{\beta\beta}=\sqrt{(z-z')^2+b^2_{\beta\beta}}$, where $b^2_{\beta\beta}=2a^2_\beta(1-\cos(\phi-\phi'))$. The approximation $R_{\alpha\beta}=b, \alpha\neq\beta$ is made for convenience, which is equivalent to the assumption of a filamentary current on conductor β, and that the field due to the current is the same on the surface of conductor α as at the center of conductor α, which is a good assumption for all $ka_\beta\ll 1$ and $b\gg a$ (for nanoradius values, there is no skin effect). In this way, $R_{\alpha\beta}\simeq\sqrt{(z-z')^2+b^2_{\alpha\beta}}, b_{\alpha\beta}=b, \alpha\neq\beta$.

Invoking the translational invariance of the structure, $I_\beta(z)=I_\beta e^{-jqz}$ and $E_z(z)=E_z e^{-jqz}$, using the relations

$$\int_{-\infty}^{\infty}e^{-jqt}\frac{1}{\sqrt{t^2+b^2}}e^{-jk\sqrt{t^2+b^2}}dt$$

$$=2K_0(b\sqrt{q^2-k^2})\times\frac{1}{2\pi}\int_0^{2\pi}K_0\left(2a_\beta\sin(\phi'/2)\sqrt{q^2-k^2}\right)d\phi' \tag{54}$$

$$=I_0(a_\beta\sqrt{q^2-k^2})K_0(a_\beta\sqrt{q^2-k^2}) \tag{55}$$

and enforcing the equations at $\phi=0$ leads to

$$Q_1I_1=I_1I_0(a_1\kappa)K_0(a_1\kappa)+I_2K_0(b_{12}\kappa)+j2\pi\omega\varepsilon E^i_{z,1} \tag{56}$$

$$Q_2I_2=I_1K_0(b_{21}\kappa)+I_2I_0(a_2\kappa)K_0(a_2\kappa)+j2\pi\omega\varepsilon E^i_{z,2}$$

where $\kappa=\sqrt{q^2-k^2}$ and

$$Q_n=\frac{j2\omega\varepsilon(1-\xi_nq^2)}{(k^2-q^2)\nu_na_n\sigma_n}=\frac{j2\omega\pi\varepsilon}{(k^2-q^2)}z \tag{57}$$

$$=\frac{j2\omega\varepsilon\pi}{(k^2-q^2)}\left(R_n+j\omega L_{n,k}+\frac{q^2}{j\omega C_{\mathrm{dos},n}}\varsigma_n\right) \tag{58}$$

where $\varsigma_n=1$ for a CNT and ς_n is given by (14) for a solid nanowire, and where I_0 and K_0 are the usual modified cylindrical Bessel functions [24]. Note that Q_n contains all information about the conductor's material properties.

The generalization to N conductors is clear,

$$I_n(Q_n-I_0(a_n\kappa)K_0(a_n\kappa))-\sum_{m=1,m\neq n}^{N}I_mK_0(b_{nm}\kappa)=j2\pi\omega\varepsilon E^i_{z,n} \tag{59}$$

$n=1,2,\ldots,N$, where b_{nm} is the center-to-center distance between conductors n and m.

In matrix form, (59) can be written as

$$\mathbf{M}(q)\mathbf{I}=[\mathbf{P}(q)-\mathbf{Q}(q)]\,\mathbf{I}=\mathbf{F}(q) \tag{60}$$

where $\mathbf{M}, \mathbf{P}$, and Q are $N\times N$ matrices (Q is a diagonal matrix with entries $Q_{nn}=Q_n$), $\mathbf{I}$ is a $N\times 1$ column of unknown current amplitudes, and $\mathbf{F}$ is a $N\times 1$ excitation column.

To determine the modal propagation constants, we solve the unforced problem (setting $E^i_z=0$). The propagation constants are determined as the complex values $q=q_p$ that force $|\mathbf{M}(q_p)|=0$. Obviously, the modal propagation constant is dependent on frequency, the system geometry, and on the material properties of each conductor.

Since $\mathbf{Q}$ is a diagonal matrix, if $Q_n=Q$ for all n (i.e., identical conductors), then we can write

$$[\mathbf{M}(q)]=[\mathbf{P}(q)-Q(q)\mathbf{1}] \tag{61}$$

where $\mathbf{P}$ is a $N\times N$ matrix that is only geometry and frequency dependent, Q is the scalar function (57) that is geometry independent, but material property dependent, and $\mathbf{1}$ is the identity matrix. Although the root q_p that forces $|\mathbf{M}(q_p)|=0$ depends on Q (and hence, on the resistance, kinetic inductance, and intrinsic capacitance of the conductors), the eigenvalues of $\mathbf{M}$ are simply the eigenvalues of $\mathbf{P}$ shifted by Q. Letting $\lambda^{(\mathbf{P})}_n$ be the eigenvalues of $\mathbf{P}$, then the eigenvalues of $\mathbf{M}$, denoted as $\lambda^{(\mathbf{M})}_n$, are simply $\lambda^{(\mathbf{M})}_n=\lambda^{(\mathbf{P})}_n-Q$. Therefore, the propagation constants, which are the zero eigenvalues of $\mathbf{M}$, can be simply obtained from the material-independent matrix $\mathbf{P}$.

A. Small Argument Approximation

Assuming that $|a_n\kappa|, |b_{n,m}\kappa|\ll 1$, we can use the small argument forms [24] $I_0(z)\simeq 1/\Gamma(1)=1, K_0(z)\simeq-\ln(z)$, leading to

$$I_n(Q_n+\ln(a_n\kappa))+\sum_{m=1,m\neq n}^{N}I_m\ln(b_{nm}\kappa)=j2\pi\omega\varepsilon E^i_{z,n} \tag{62}$$

for $n=1,2,3,\ldots,N$.

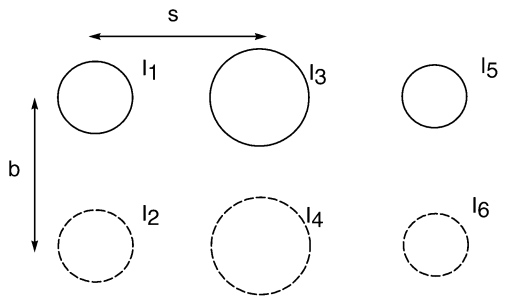

Fig. 2. Two rows of conductors with odd current symmetry in the vertical direction (e.g., conductors over a ground plane, or two rows of conductors carrying a transmission line mode current) (i.e., having odd symmetry in the vertical direction).

At this point it is useful to consider an array with a symmetry plane, such as a row of conductors above a ground plane or two rows of conductors carrying currents with odd symmetry in the vertical direction, as depicted in Fig. 2. If we number the conductors as indicated in this figure and enforce $I_2 = -I_1, I_4 = -I_3, I_6 = -I_5$, etc., we obtain

$$I_n\left(\ln\left(\frac{b}{a_n}\right) - Q_n\right) + \sum_{m=1,3,5,\ldots m\neq n}^{N} I_m \ln\left(\frac{b_{n,m+1}}{b_{n,m}}\right) = -j2\pi\omega\varepsilon E^i_{z,n} \quad (63)$$

for $n = 1, 3, 5, \ldots, N$. In matrix form, this can be written as

$$\mathbf{M}(q)\mathbf{I} = [\mathbf{P} - \mathbf{Q}(q)]\mathbf{I} = \mathbf{F}(q). \quad (64)$$

Importantly, the matrix $\mathbf{P}$ is now independent of q and frequency, and only depends on geometry.

For identical nanotubes, we have

$$[\mathbf{M}(q)] = [\mathbf{P} - Q(q)\mathbf{1}]. \quad (65)$$

The propagation constants q_n are determined from $\lambda_n^{(\mathbf{M})} = 0 = \lambda_n^{(\mathbf{P})} - Q$, leading to the propagation values

$$q_{p,n} = \sqrt{\frac{\nu a\sigma(\omega)k^2\lambda_n^{(\mathbf{P})} - j2\omega\varepsilon}{\nu a\sigma(\omega)\lambda_n^{(\mathbf{P})} - j2\omega\varepsilon\xi}}. \quad (66)$$

Thus, the dispersive fundamental material-dependent propagation constants can be obtained without a root search in the complex plane, and are given analytically in terms of the static eigenvalues of the matrix $\mathbf{P}$, which only depends on geometry. The smallest eigenvalue $n = 1$ is associated with the dominant mode of propagation.

For the special case of two conductors, $\lambda^{(\mathbf{P})} = \ln(b/a)$, such that

$$\frac{q_p}{k_0} = \sqrt{\frac{1 + \frac{2L_k}{L_E}\left(1 + \frac{1}{j\omega t}\right)}{1 + \frac{C_E}{C_{\rm dos}/2}}} \quad (67)$$

where $L_E = \mu\ln(b/a)/\pi$ and $C_E = \pi\varepsilon/\ln(a/b)$ are the electrostatic inductance and capacitance, respectively, of a two-conductor configuration. If spatial dispersion is ignored, the term $C_E/C_{\rm dos}$ is absent. As discussed later, the factors of 2 are because L_k and $C_{\rm dos}$ are intrinsic to each conductor, and there are two conductors.

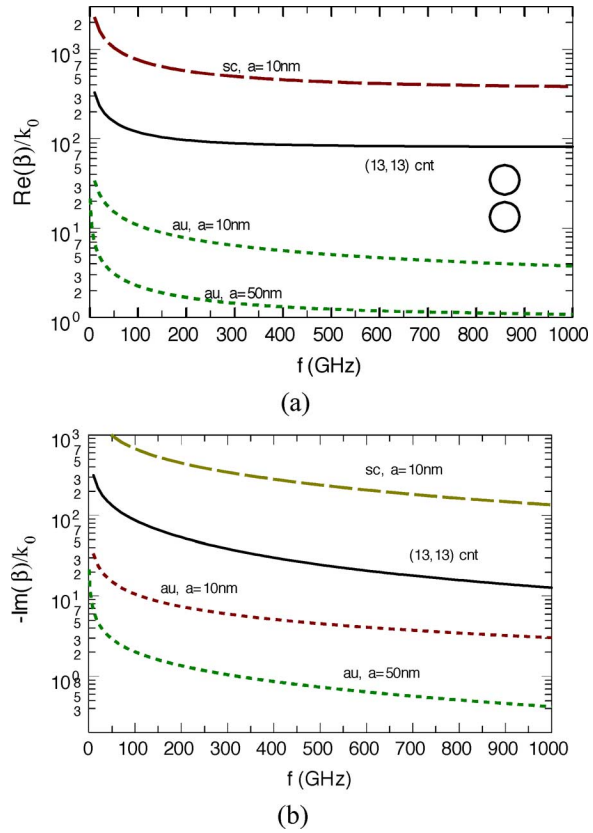

Fig. 3. (a) $\mathrm{Re}(\beta)/k_0$ versus frequency for a two-conductor array. Several conductor types are shown—solid gold nanowires having $a = 50$ nm and $a = 10$ nm, a degenerately doped GaAs nanowire ($\sigma_0 \sim 10^4$ S/m, $\tau \sim 2 \times 10^{-13}$ s) having $a = 10$ nm, and a (13,13) CNT. (b). Same as Fig. 3(a), except for $\mathrm{Im}(\beta)/k_0$.

In the following, we consider two- and four-conductor array geometries having $b/a = s/a = 11.35$ for the case of conductors in free space having currents with odd symmetry in the vertical direction (i.e., a transmission line mode of the structure). For the (13,13) nanotubes considered here, which have radius $a = 0.8814$ nm, this corresponds to vertical and horizontal separation $b = s = 10$ nm. For $a = 10$ nm nanowires, this corresponds to $b = s = 113.5$ nm, and for $a = 50$ nm nanowires, $b = s = 567.3$ nm. In the following, we rename the propagation constant q_p as β.

Fig. 3(a) and (b) shows $\mathrm{Re}(\beta)/k_0$ and $\mathrm{Im}(\beta)/k_0$ versus frequency for the fundamental mode of a two-conductor array. We consider $a = 50$ nm and $a = 10$ nm au nanowires, a (13,13) CNT, and a degenerately doped GaAs nanowire ($\sigma_0 \sim 10^4$ S/m, $\tau \sim 2 \times 10^{-13}$ s) having $a = 10$ nm (we ignore radial quantization). All results include spatial dispersion, but since ignoring spatial dispersion only changes the results for the CNT and semiconducting nanowire by a few percent (e.g., $(1 + 2C_E/C_{\rm dos})^{1/2}_{\rm cnt} \simeq 1.035$ and, at $a = 10$ nm, $(1 + 2C_E/C_{\rm dos})^{1/2}_{\rm sc} \simeq 1.049$), and much less than 1% for the metal nanowire (at $a = 10$ nm $(1 + 2C_E/C_{\rm dos})^{1/2}_{\rm au} \simeq 1$), setting $\xi = 0$ would not noticeably affect the plot given the

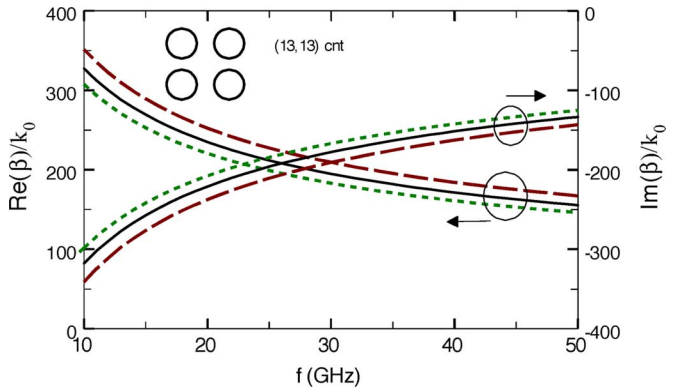

Fig. 4. Propagation constants β/k_0 for a four-nanotube array of (13,13) CNTs. The center curve is the two-conductor result (two tubes vertically aligned).

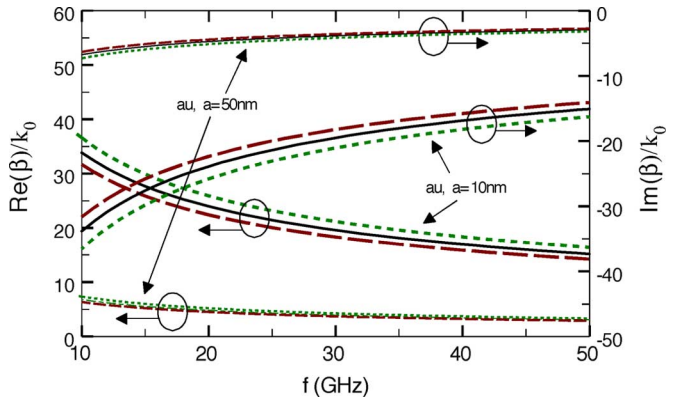

Fig. 5. Propagation constants β/k_0 for a four-nanowire array of gold nanowires. The center curve is the two-conductor result (two nanowires vertically aligned).

scale of the vertical axis. It can be seen that propagation along the au nanowires is much faster than on the other structures, with much less attenuation.

In Fig. 4, fundamental propagation constants for a four-conductor array (two rows of conductors having currents with odd symmetry in the vertical direction) is shown for (13,13) CNTs. The center curve is the two-conductor result, and the two surrounding curves are the four-conductor case (forming even and odd modes of propagation). It can be seen that, at several tens of GHz, the four-nanotube modes coalesces into the two-nanotube case. The local approximation ($\xi = 0$) is not shown for the sake of clarity, but it would result in a noticeable shift of the curves ($\simeq 3.5\%$). Similarly, although not shown, for a GaAs nanowire the local and nonlocal results differ by approximately 5%, and for lower doping levels nonlocality becomes even more important for semiconducting nanowires (e.g., if $\sigma_0 = 10^3$ S/m there is a 10% shift between local and nonlocal results, $(1 + 2C_E/C_{\rm dos})^{1/2}_{\rm sc} \simeq 1.10$).

Fig. 5 shows propagation constants for a four-conductor array of au nanowires for both $a = 10$ nm and $a = 50$ nm. Clearly, the thicker nanowires exhibit less separation between even and odd modes (recall that the conductor spacing is larger for the $a = 50$ nm conductors).

V. Multiconductor Transmission Line (MTL) Theory

In this section, the per-unit-length transmission line parameters are obtained from the coupled integral equations (63) for a system of two rows of conductors with odd current symmetry in the vertical direction. If we define $\mathbf{L} = (\mu/\pi)\mathbf{P}$ (this definition is consistent with [25], although the $\mathbf{P}$ used here and in that reference differ by a factor of $\pi\varepsilon$), then (64) can be written as

$$\left[\mathbf{L} - \frac{\mu}{\pi}\mathbf{Q}\right]\mathbf{I} = \frac{\mu}{\pi}\mathbf{F} \tag{68}$$

where Q is a diagonal matrix with entries

$$Q_{nn} = \frac{j2\omega\varepsilon\left(1 - \xi_n q^2\right)}{(k^2 - q^2)\nu_n a_n \sigma_n}. \tag{69}$$

Using $z(q,\omega) = 1/\pi\nu_n a_n \sigma_n(q,\omega)$ and (6), (68) can be written as

$$\left[\mathbf{L} - \frac{j2\omega\varepsilon\mu(1 - \xi_n q^2)}{(k^2 - q^2)} z_n \mathbf{1}\right]\mathbf{I} = \frac{\mu}{\pi}\mathbf{F}. \tag{70}$$

With $\mathbf{C}^{-1} = \mathbf{L}/\mu\varepsilon$ for homogeneous media and (3), we have

$$\left[\omega^2(\mathbf{L} + \mathbf{L}_k) - q^2\left(\mathbf{C}^{-1} + \mathbf{C}_{\rm dos}^{-1}\right) - j\omega\mathbf{R}\right]\mathbf{I} = \frac{\left(k^2 - q^2\right)}{\varepsilon\pi}\mathbf{F} \tag{71}$$

where $\mathbf{R}, \mathbf{C}_{\rm dos}$, and $\mathbf{L}_k$ are diagonal matrices with $\mathbf{L}_k = 2L_{k,n}\mathbf{1}, \mathbf{C}_{\rm dos} = (C_{\rm dos,n}/2\varsigma_n)\mathbf{1}$, and the ohmic resistance diagonal matrix $\mathbf{R}$ has entries $2R_n$ (all matrices are per-unit-length quantities). Note that this result is for two rows of nanotubes having currents with odd symmetry in the vertical direction. The factor of 2 in $\mathbf{R}$ reflects the fact that the current flows through a conductor in one row and also through its return in the other row. Since R is the resistance of each conductor, the total resistance is $2R$ (note that this is consistent with the usual transmission line formulation, where, e.g., $\mathbf{R}$ is the total resistance of both conductors). Since L_k and $C_{\rm dos}$ are similarly intrinsic to the conductors, the factors of 2 and 1/2 in $\mathbf{L}_k$ and $\mathbf{C}_{\rm dos}$, respectively, are due to the same reason. For conductors above a perfect ground plane, we would remove the factors of 2 since the return row of conductors (i.e., the ground plane) does not exhibit R, L_k, and $C_{\rm dos}$.

Equation (71) can be written as $(d^2/dz^2 - \mathbf{YZ})\mathbf{I} = \mathbf{0}$, where the admittance and impedance matrices are $\mathbf{Y} = j\omega\mathbf{C}, \mathbf{Z} = \mathbf{R} + j\omega\mathbf{L}$, which is the usual MTL formulation for the unforced problem [25].

Note that we have obtained the total capacitance as the series combination of the electrostatic and intrinsic (quantum) capacitance matrices, which is a generalization to the usual scalar transmission line result [1]. Being a series combination, the intrinsic capacitance acts to reduce the total capacitance from the electrostatic value. This reduction of capacitance due to the finite density of states makes sense if one considers the energy (W) charge (Q) relationship $W = Q^2/2C$. For a material with an infinite density of states (i.e., a perfect conductor), we can consider all of the charge to reside at the bottom of the conduction band. If the material has a finite density of states, we need to apply more energy to get the same charge since we need to fill in higher energy states. The requirement of needing more

energy to produce the same charge is equivalent to reducing the capacitance since $W = Q^2/2C$. Here we ignore electron exchange-correlation energies [26].

Also, note that if $\sigma \to \infty$, it would appear that $Q \to 0$ and we are left with only an inductance matrix. However, in that case we have a pure TEM mode, and $q = k$ such that Q remains finite and we recover the correct transmission line result. Transmission line analysis of single CNTs and quantum wires above a ground plane have been given in [1], [3], [4], and [27], among others.

It is worth noting that using the homogeneous system of integral equations cast into the homogeneous form of (71) and comparing with the standard MTL equations, one can only identify the relative values of R, L, and C up to a constant. For example, for two wires without a ground plane, (71) becomes

$$\omega^2\left(\frac{\mu}{\pi}\ln\left(\frac{b}{a}\right)+2L_{c1}\right)-q^2\left(\left(\frac{\pi\varepsilon}{\ln\left(\frac{b}{a}\right)}\right)^{-1}+\left(\frac{C_q}{2}\right)^{-1}\right)-j\omega 2R_{c1}=0. \quad (72)$$

The first term is the electrostatic inductance for the two-wire geometry, and the third term is the electrostatic capacitance for the two-wire geometry. For the case of a ground plane, it is convenient to divide the above equation by 2 such that the first term is the electrostatic inductance for a wire above a ground plane, the second term has one factor of L_{c1}, the third term is the electrostatic capacitance for a wire above the ground plane, the fourth term is the quantum capacitance of one wire above a ground plane, and the last term is the resistance associated with one wire. Obviously, one can multiply (72) by any constant. Thus, one cannot use the integral equation method in the homogeneous case to identify the values of R, L, and C since one only obtains the relative values for a given geometry.

The formulation presented here serves as an extension of the classical MTL formulation developed for macroradius conductors to nanoradius conductors.

VI. Conclusion

A general formulation has been presented for the spatially dispersive conductivity, distributed impedance, Ohm's law relation, and transmission line model of both single-wall CNTs and solid material nanowires. Spatial dispersion, which results in an intrinsic (material-dependent) distributed capacitance, is shown to be theoretically important in all structures, and numerically important in CNTs and solid lower conductivity nanowires (including doped semiconducting nanowires), but unimportant in highly conducting metal nanowires.

Appendix
Derivation of Conductivity, Generalized Ohm's Law, Distributed Impedance, and Integral Equation

In this appendix, the new results presented in the body of the paper are derived, excepting the transmission-line model, which was presented in the previous section. The role of diffusion is highlighted in obtaining the correct spatial dispersion relation and associated intrinsic capacitance.

To obtain (1), (3), (4), and (7), we start with Boltzmann's transport equation [18]

$$\frac{\partial f}{\partial t}+\mathbf{v}\cdot\nabla_{\mathbf{r}}f-\frac{e}{\hbar}\left(\mathbf{E}(\mathbf{r},t)+\mathbf{v}\times\mathbf{B}(\mathbf{r},t)\right)\cdot\nabla_{\mathbf{k}}f=\left(\frac{\partial f}{\partial t}\right)_{\text{coll}} \quad (73)$$

where $f = f(\mathbf{r},\mathbf{k},t)$ is the phase–space electron distribution function (i.e., the probability of finding an electron at position $\mathbf{r}=\mathbf{r}(t)$ at time t, and having quasi-momentum $\hbar\mathbf{k}=\hbar\mathbf{k}(t)$),

$$\mathbf{v}=\frac{d\mathbf{r}}{dt}=\mathbf{v}(\mathbf{k})=\frac{1}{\hbar}\nabla_{\mathbf{k}}\varepsilon(\mathbf{k}) \quad (74)$$

is the electron velocity, $\varepsilon(\mathbf{k})$ is the electron energy, and

$$\mathbf{F}(\mathbf{r},t)=-\frac{e}{\hbar}(\mathbf{E}(\mathbf{r},t)+\mathbf{v}\times\mathbf{B}(\mathbf{r},t))=\hbar\frac{d\mathbf{k}}{dt} \quad (75)$$

is the force on the electron.

In the usual RTA, the collision integral is [18]

$$\left(\frac{\partial f}{\partial t}\right)_{\text{coll}}=-\frac{f-f_0}{\tau} \quad (76)$$

where f_0 is the equilibrium Fermi distribution

$$f_0=\left(e^{(\varepsilon-\mu)/k_BT}+1\right)^{-1} \quad (77)$$

evaluated at energy ε and chemical potential μ. This collision term implies that collisions return the system to global equilibrium (exponentially) in time τ. However, this approximation does not conserve particle number [29, p. 313], [18, problem 13.4], [30], and leads to a quantum capacitance that diverges at low frequency. Here we use the collision ansatz (sometimes called the Bhatnager–Gross–Krook (BGK) model) [29], [31]

$$\left(\frac{\partial f}{\partial t}\right)_{\text{coll}}=-\frac{f-f_s}{\tau} \quad (78)$$

where f_s is a local equilibrium distribution function after scattering. In this case, collisions do not return the system to equilibrium, but to a state described by f_s, slightly perturbed from equilibrium. It was found that this method leads to the same result as the well-known Mermin correction that conserves particle number, which is typically applied to the Lindhard permittivity [32]) (see [33] for the hydrodynamic case for an electron gas). For a metal, the spatially dispersive conductivity is given in [34]; however, there the authors use (76), and thus, charge conservation is not enforced.

We assume $f = f_0 + f_1$ with $f_1 \ll f_0$ and that f_s belongs to the same local particle density as does f. We write the local equilibrium distribution as a small perturbation of the Fermi distribution, $f_s = f_0 + h$, where $h \ll f_0$ so that the collision term becomes

$$\left(\frac{\partial f}{\partial t}\right)_{\text{coll}}=-\frac{f_1-h}{\tau}. \quad (79)$$

We assume that a small electric field $E_0 e^{-jqz}$ perturbs the distribution from its equilibrium value. The change in the electron distribution is via the electron density

$$n(z) = n_0 + n_1 e^{-jqz} \tag{80}$$

where n_0 is the equilibrium density and $n_1 \ll n_0$ is the induced density that varies as the applied field. This, in turn, produces a perturbation in the chemical potential $\mu = \mu(n(z)) = \mu^0 + \delta\mu e^{-jqz}$, where $\mu^0 = 0$ for CNTs. Because the local equilibrium distribution will have the same general form as the Fermi distribution, we expand the distribution f_s in terms of the equilibrium value

$$f_s \simeq f_0 + \frac{\partial f_0}{\partial n} n_1 e^{-jqz} = f_0 + \frac{\partial f_0}{\partial \mu}\frac{\partial \mu}{\partial n} n_1 e^{-jqz} \tag{81}$$

where $f_0 = f_0(\mu(n))$. In the RTA (76), the collision term becomes $(\partial f/\partial t)_{\text{coll}} = -f_1/\tau$, whereas in (78), we have $(\partial f/\partial t)_{\text{coll}} = -(f_1 - h)/\tau$. It is the presence of h that allows an extra degree of freedom to enforce continuity, as shown below (in this case, by the proper choice of n_1), which is not possible in the approximation (76).

The equilibrium density satisfies

$$\frac{\partial f_0}{\partial t} + \mathbf{v}\cdot\nabla_{\mathbf{r}} f_0 = 0 \tag{82}$$

and, replacing $\partial/\partial t \to j\omega$, ignoring the small magnetic field contribution, and keeping only first-order terms

$$j f_1(\omega - \mathbf{v}\cdot\mathbf{q} - j\tau^{-1}) - \frac{e}{\hbar}\mathbf{E}\cdot\frac{\partial f_0}{\partial \varepsilon}\hbar\mathbf{v} = \frac{h}{\tau}$$

where we used $\mathbf{v}(\mathbf{k}) = (1/\hbar)\nabla_{\mathbf{k}}\varepsilon(\mathbf{k})$. Ignoring the small magnetic field contribution, we obtain

$$f_1 = \frac{-jh\tau^{-1}}{(\omega - \mathbf{v}\cdot\mathbf{q} - j\tau^{-1})} - \frac{je\mathbf{E}\cdot\mathbf{v}}{(\omega - \mathbf{v}\cdot\mathbf{q} - j\tau^{-1})}\frac{\partial f_0}{\partial \varepsilon}. \tag{83}$$

The current density in the Fourier transform domain is (the 2 in the numerator accounts for spin)

$$\begin{aligned}\mathbf{J}(\mathbf{q},\omega) &= -2e\int \mathbf{v}(\mathbf{k}) f_1 d\mathbf{k} \\ &= j2e\int \mathbf{v}(\mathbf{k})\left(\frac{h\tau^{-1} + e\mathbf{E}(\mathbf{q},\omega)\cdot\mathbf{v}(\mathbf{k})\frac{\partial f_0}{\partial \varepsilon}}{\omega - \mathbf{v}\cdot\mathbf{q} - j\tau^{-1}}\right) d\mathbf{k}\end{aligned} \tag{84}$$

since no current flows from the equilibrium distribution, where

$$\begin{aligned} d\mathbf{k} &= \frac{dk_x dk_y dk_z}{(2\pi)^3} = dk d\Omega \\ d\Omega &= \frac{k^2 \sin\theta d\theta d\phi}{(2\pi)^3} \quad \text{solid nanowire} \end{aligned} \tag{85}$$

$$d\mathbf{k} = dk_z d\Omega \quad d\Omega = \frac{dk_\perp}{(2\pi)^2} \quad \text{CNT}. \tag{86}$$

For the electrically thin structures of interest here, we can approximate the current as flowing in the z direction. Let $\mathbf{J}(\mathbf{q},\omega) = \mathbf{z}J_z(q,\omega), \mathbf{v}(\mathbf{k}) = \mathbf{z}v_z(\mathbf{k}), \mathbf{E}(\mathbf{q},\omega) = \mathbf{z}E_z(q,\omega)$, and $\mathbf{q} = \mathbf{z}q$ such that

$$J_z(q,\omega) = j2e\int\left(\frac{v_z(\mathbf{k})h\tau^{-1} + ev_z^2(\mathbf{k})\frac{\partial f_0}{\partial \varepsilon}E_z(q,\omega)}{\omega - v_z(\mathbf{k})q - j\tau^{-1}}\right) d\mathbf{k}. \tag{87}$$

Since $\tau^{-1} \gg \omega, v_z q$, Landau damping is not an issue.

We need to enforce continuity by the proper choice of n_1. We have

$$\nabla\cdot\mathbf{J} = -j\omega\rho \tag{88}$$

$$-jqJ_z = j\omega e n_1 \tag{89}$$

$$n_1 = \frac{-qJ_z}{\omega e} \tag{90}$$

where J_z is A/m^2, and for a CNT (J_z is A/m)

$$n_1^{cnt} = \frac{-2\pi r_{cn} q J_z}{\omega e}. \tag{91}$$

Writing $h = (\partial f_0/\partial\mu)\alpha n_1 e^{-jqz} = -(\partial f_0/\partial\varepsilon)\alpha n_1 e^{-jqz}$, where $\alpha = \partial\mu/\partial n$, suppressing e^{-jqz} common to all terms, and using

$$\frac{1}{\omega - v_z q - i\tau^{-1}} = \frac{1}{(\omega - i\tau^{-1})}\sum_{n=0}^{\infty}\frac{q^n v_z^n}{(\omega - i\tau^{-1})^n} \tag{92}$$

which converges for $|x| < 1$, where $x = qv_z/(\omega - i\tau^{-1})$, we have

$$J_z(q,\omega)\left(1 - \frac{j2\beta\alpha\tau^{-1}}{\omega}\sum_{n=1}^{\infty}\frac{q^n}{(\omega - i\tau^{-1})^n}\int v_z^n(k)\frac{\partial f_0}{\partial\varepsilon}d\mathbf{k}\right) \tag{93}$$

$$= \left(j2e^2\sum_{n=1}^{\infty}\frac{q^{n-1}}{(\omega - i\tau^{-1})^n}\int v_z^{n+1}(k)\frac{\partial f_0}{\partial\varepsilon}d\mathbf{k}\right) E_z(q,\omega) \tag{94}$$

where $\beta = 1$ for solid nanowires and $\beta = 2\pi r_{cn}$ for CNTs. Since $v_z(-k_z) = -v_z(k_z)$ for materials with parabolic (metals) or linear (CNT) energy bands, then

$$J_z(q,\omega)\left(1 - \frac{j2\beta\alpha\tau^{-1}}{\omega}\right. \tag{95}$$

$$\left.\times\sum_{n=2,4,6,\ldots}^{\infty}\frac{q^n}{(\omega - i\tau^{-1})^n}\int v_z^n(k)\frac{\partial f_0}{\partial\varepsilon}d\mathbf{k}\right) \tag{96}$$

$$= \left(j2e^2\int\frac{v_z^2}{(\omega - i\tau^{-1})}\right. \tag{97}$$

$$\left.\times\sum_{n=1,3,5,\ldots}^{\infty}\left(\frac{qv_z}{(\omega - i\tau^{-1})}\right)^{n-1}\frac{\partial f_0}{\partial\varepsilon}d\mathbf{k}\right) E_z(q,\omega). \tag{98}$$

For the right-side term, we note

$$\sum_{n=1,3,5,\ldots}^{\infty} x^{n-1} = \sum_{n=0}^{\infty} x^{2n} = \frac{1}{1-x^2} \tag{99}$$

and for the left-side term,

$$\sum_{n=2,4,6,\ldots}^{\infty} x^{n} = x^2 \sum_{n=0.}^{\infty} x^{2n} = \frac{x^2}{1-x^2}. \tag{100}$$

Therefore,

$$J_z(q,\omega)\left(I(q,\omega)^{-1} - \frac{j2\beta\alpha\tau^{-1}q^2}{\omega(\omega - i\tau^{-1})^2}\right) = \frac{j2e^2}{(\omega - i\tau^{-1})}\, E_z(q,\omega) \tag{101}$$

where

$$I(q,\omega) = \int \frac{v_z^2}{1 - \left(\frac{qv_z}{(\omega - i\tau^{-1})}\right)^2} \frac{\partial f_0}{\partial \varepsilon} d\mathbf{k} \tag{102}$$

so that

$$\sigma(q,\omega) = \frac{j2e^2}{(\omega - i\tau^{-1})}\left(I(q,\omega)^{-1} - \frac{j2\beta\alpha\tau^{-1}q^2}{\omega(\omega - i\tau^{-1})^2}\right)^{-1} \tag{103}$$

which is (1).

Although it is not necessary, it is convenient to assume $T = 0$ K since then $\partial f_0/\partial\varepsilon = -\delta(\varepsilon - \varepsilon_F)$. For metals and metallic CNTs, we can use this approximation for all temperatures. We can therefore write $v_z = v_F g(\theta)$ (e.g., in three dimensions $v_z = v_F \cos\theta$ and for a quasi-1-D structure like a CNT, $g = 1$ and $v_z = v_F$). Using $dk = d\varepsilon/\hbar v \to d\varepsilon/\hbar v_F$, we have

$$I(q,\omega) = -\frac{v_F}{\hbar}\int \frac{g^2(\theta)}{1 - \left(\frac{qv_F g(\theta)}{(\omega - i\tau^{-1})}\right)^2} d\Omega \tag{104}$$

and so

$$J_z(q,\omega)\left(\left(\int \frac{g^2(\theta)}{1 - \left(\frac{qv_F g(\theta)}{(\omega - i\tau^{-1})}\right)^2} d\Omega\right)^{-1} + \frac{j2\beta\alpha v_F \tau^{-1} q^2}{\hbar\omega(\omega - i\tau^{-1})^2}\right) \tag{105}$$

$$= \frac{-j2e^2 v_F}{\hbar(\omega - i\tau^{-1})}\, E_z(q,\omega) \tag{106}$$

such that

$$\sigma(q,\omega) = \frac{-j2e^2 v_F}{\hbar(\omega - i\tau^{-1})}\left(I_1(q,\omega)^{-1} + \frac{j2\beta\alpha\tau^{-1}q^2 v_F}{\hbar\omega(\omega - i\tau^{-1})^2}\right)^{-1} \tag{107}$$

where

$$I_1(q,\omega) = \int \frac{g^2(\theta)}{1 - \left(\frac{qv_F g(\theta)}{(\omega - i\tau^{-1})}\right)^2} d\Omega. \tag{108}$$

In order to obtain (4), write $b = qv_F/(\omega - i\tau^{-1})$ and use

$$\int \frac{g^2(\theta)}{1 - b^2 g^2(\theta)} d\Omega = \int g^2(\theta) \sum_{n=0}^{\infty} (bg(\theta))^{2n} d\Omega \tag{109}$$

$$= \sum_{n=0}^{\infty} b^{2n} \int g^{2n+2}(\theta) d\Omega = \sum_{n=0}^{\infty} b^{2n} a_{2n} \tag{110}$$

$$= a_0 + a_2 b^2 + a_4 b^4 + \cdots \tag{111}$$

where $a_{2n} = \int g^{2n+2}(\theta) d\Omega$. Therefore,

$$\frac{J_z(q,\omega)}{\int \frac{g^2(\theta)}{1 - b^2 g^2(\theta)} d\Omega} = \frac{J_z(q,\omega)}{\sum_{n=0}^{\infty} b^{2n} a_{2n}} \simeq \frac{J_z(q,\omega)}{a_0\left(1 + \frac{a_2}{a_0} b^2\right)} \tag{112}$$

$$\simeq \frac{1}{a_0} J_z(q,\omega)\left(1 - \frac{a_2}{a_0} b^2\right) \tag{113}$$

leading to

$$J_z(q,\omega)\left(1 - \left(\frac{a_2}{a_0} - \frac{j2\beta\alpha\tau^{-1}a_0}{\omega\hbar v_F}\right)\left(\frac{qv_F}{(\omega - i\tau^{-1})}\right)^2\right) \tag{114}$$

$$= \frac{-j2e^2 a_0 v_F}{\hbar(\omega - i\tau^{-1})}\, E_z(q,\omega) \tag{115}$$

which has the form (4) with

$$\xi = \left(\frac{a_2}{a_0} - \frac{j2\beta\alpha\tau^{-1}a_0}{\omega\hbar v_F}\right)\left(\frac{v_F}{(\omega - i\tau^{-1})}\right)^2 \tag{116}$$

and

$$\sigma(\omega) = \frac{-j2e^2 a_0 v_F}{\hbar(\omega - i\tau^{-1})}. \tag{117}$$

Note that if all a_{2n} values are equal (which occurs for CNTs, but not for solid nanowires), than the series $\sum_{n=0}^{\infty} b^{2n} a_{2n}$ can be summed in closed form and the approximate equal signs in (112) become equalities. In this case, there is only quadratic spatial dispersion.

As an example, for a solid nanowire ($\beta = 1, g(\theta) = \cos\theta, d\Omega = k^2 \sin\theta d\theta d\phi/(2\pi)^3$),

$$a_0 = \frac{k_F^2}{(2\pi)^3}\int_0^{2\pi} d\phi \int_0^{\pi} \cos^2\theta \sin\theta d\theta = \frac{4}{3}\pi\frac{k_F^2}{(2\pi)^3} \tag{118}$$

$$a_2 = \frac{k_F^2}{(2\pi)^3}\int_0^{2\pi} d\phi \int_0^{\pi} \cos^4\theta \sin\theta d\theta = \frac{4}{5}\pi\frac{k_F^2}{(2\pi)^3}. \tag{119}$$

Equation (116) then leads to (13). Since

$$\mu = \varepsilon_F = \frac{\hbar^2}{2m} k_F^2 = \left(3n\frac{\hbar^3\pi^2}{(2m)^{3/2}}\right)^{2/3} \tag{120}$$

$$\alpha = \frac{\partial \varepsilon_F}{\partial n} = \left(3\frac{\hbar^3\pi^2}{(2m)^{3/2}}\right)^{2/3}\frac{2}{3}n^{-1/3} \tag{121}$$

we find that $\alpha k_F = \hbar^2\pi^2/m$, leading to $\sigma(\omega) = \sigma_0/(1+j\omega\tau)$, where $\sigma_0 = e^2\tau N/m$ is the usual dc conductivity. The integral

$$\int \frac{\cos^2(\theta)\sin\theta}{1-b^2\cos^2\theta}d\theta = \frac{-2}{b^2}\left(1+\frac{1}{2b}\ln\left(\frac{1-b}{1+b}\right)\right) \tag{122}$$

used in (107) leads to (11). If we do not enforce charge continuity [i.e., if we use (76)], the term $-j/\omega\tau$ is missing in (11), and instead of (13), we obtain

$$\xi_{\rm RTA}^{\rm solid} = \frac{3}{5}\left(\frac{v_F\tau}{1+j\omega\tau}\right)^2 \tag{123}$$

which does not lead to $C_{\rm dos}$ such that $L_kC_{\rm dos} = 1/v_F^2$.

For a CNT, $g(\theta) = 1, \beta = 2\pi a$, and $d\Omega = dk_\perp/(2\pi)^2$. The double integral over the tube length and circumference $C = 2\pi a$ is evaluated as [5], [16]

$$\int dk_z \int dk_\perp\, f(k_z,k_\phi) = \int dk_z \frac{2\pi}{C}\sum_\mu f(k_z,\mu) \tag{124}$$

where μ is a discrete index that accounts for azimuthal quantization of the electron wave function. Then

$$a_{2n} = \int d\Omega = \frac{1}{(2\pi)^2}\int dk_\phi = \frac{1}{(2\pi)^2 a}\sum_\mu \tag{125}$$

$$= \frac{1}{(2\pi)^2 a}(2)(2) = \frac{1}{\pi^2 a} \tag{126}$$

where the first 2 is for the contribution of holes and the second 2 is for having two inequivalent Fermi points (valley degeneracy of two). Using [35],

$$\alpha = \frac{\partial\varepsilon_F}{\partial n} = \frac{e^2}{C_{\rm dos}} = \frac{hv_F}{8} \tag{127}$$

we then have (18) and (19) and $\sigma(\omega) = -j2e^2v_F/\pi^2 a\hbar(\omega - i\tau^{-1})$. The conductivity (107) leads to (18), and (116) provides (20). If we do not enforce charge continuity (i.e., without diffusion), we obtain

$$\xi_{\rm RTA}^{\rm cnt} = \frac{v_F^2\tau^2}{(1+j\omega\tau)^2} \tag{128}$$

which does not lead to the quantum capacitance $C_{\rm dos} = C_q = 8e^2/hv_F$, nor does it provide $L_kC_{\rm dos} = 1/v_F^2$.

The distributed impedance (Ω/m) is easily obtained. For a solid nanowire, using (11) we have

$$z_m = \frac{1}{\pi a^2\sigma(q,\omega)} = R^{\rm solid} + j\omega L_k^{\rm solid} \tag{129}$$

$$+ R^{\rm solid}\left(\frac{3}{5} - \frac{j}{3\omega\tau}\right)\frac{v_F^2\tau^2}{(1+j\omega\tau)}q^2 \tag{130}$$

where

$$R^{\rm solid} = \frac{1}{\pi a^2\sigma_0} \quad L_k^{\rm solid} = \tau R^{\rm solid}. \tag{131}$$

Using $\alpha = \partial\varepsilon_F/\partial n = e^2/\tilde{C}_{\rm dos}$, we obtain

$$\tilde{C}_{\rm dos} = \frac{3me^2}{(3\hbar^3\pi^2)^{2/3}}n^{1/3}. \tag{132}$$

Redefining $C_{\rm dos} = \tilde{C}_{\rm dos}\pi a^3/3$ leads to (15). Noting

$$v_F^2 = \frac{2}{m}\varepsilon_F = \frac{1}{m^2}(3N\hbar^3\pi^2)^{2/3} \tag{133}$$

leads to $L_k^{\rm solid}C_{\rm dos}^{\rm solid} = 1/v_F^2$. In a similar manner, using (18) for a CNT, the distributed impedance (Ω/m) $z_{cn}(q,\omega) = 1/2\pi a\sigma(q,\omega)$ is easily found to be (21). In all structures, if spatial dispersion is ignored, the intrinsic capacitance $C_{\rm dos}$ would be missing.

To derive integral equation (7), note that, in a homogeneous space, the electric field-electric current density relationship is [36]

$$\mathbf{E}(\mathbf{r}) = \frac{1}{j\omega\varepsilon}\left(k^2 + \boldsymbol{\nabla}\boldsymbol{\nabla}\cdot\right)\int_\Omega \frac{e^{-jkR(\mathbf{r},\mathbf{r}')}}{4\pi R(\mathbf{r},\mathbf{r}')}\mathbf{J}(\mathbf{r}')d\mathbf{r}' \tag{134}$$

where $R(\mathbf{r},\mathbf{r}') = |\mathbf{r}-\mathbf{r}'|, \mathbf{J}$ is a 3-D current density (A/m^2) and Ω is the support of the current. For an electrically thin solid metal $I(z) = J_z(z)\pi a^2$, where J_z has units A/m^2, and for a CNT $\mathbf{J}(\mathbf{r}) = \hat{\mathbf{z}}J_z(z)\delta(\rho - a)$, where J_z is a surface current (A/m) so that $I(z) = J_z(z)2\pi a$. We can write this generally as $I(z) = J_z(z)\nu\pi a$, where $\nu = 2$ for a CNT and $\nu = a$ for a solid cylinder. We have assumed that the current density is independent of angle ϕ around the tube, which is a reasonable assumption since $ka \ll 1$ through optical frequencies. In this case,

$$E_z(z,\phi) = \frac{1}{j4\pi\omega\varepsilon}\left(k^2 + \frac{\partial^2}{\partial z^2}\right)I(\rho,\phi,z,\rho') \tag{135}$$

where

$$I(\rho,\phi,z,\rho') = \int_{-\infty}^{\infty}\int_{-\pi}^{\pi}\frac{e^{-jkR}}{R}\frac{I(z')}{2\pi}d\phi' dz' \tag{136}$$

(the 2π emerges for both tubes and solid cylinders since for tubes we have $\int J_z\delta(\rho-a)\rho d\rho = (I/2\pi a)a = I/2\pi$ and for solid cylinders we have $\int J_z\rho d\rho = (I/\pi a^2)a^2/2 = I/2\pi$) and where $R(\rho,\phi,z,\rho',\phi',z') = \sqrt{(z-z')^2+b^2}, b^2 = (\rho\cos\phi - \rho'\cos\phi')^2 + (\rho\sin\phi - \rho'\sin\phi')^2$.

Considering a single conductor and using (4) with the total electric field being the electric field due to current on the conductor (135), plus a possible incident field E_z^i, we obtain the integral equation (7)

$$\left(1 + \xi\frac{\partial^2}{\partial z^2}\right)\frac{I(z)}{\nu\pi a\sigma(\omega)} \tag{137}$$

$$= \frac{1}{j4\pi\omega\varepsilon}\left(k^2 + \frac{\partial^2}{\partial z^2}\right)I(\rho,\phi,z,\rho') + E_z^i \tag{138}$$

for all $-\pi \le \phi \le \pi, -\infty < z < \infty$, where $\rho, \rho' = a$.

ACKNOWLEDGMENT

The author would like to thank the anonymous reviewers for helpful comments concerning this problem.

REFERENCES

[1] P. J. Burke, "An RF circuit model for carbon nanotubes," *IEEE Trans. Nanotechnol.*, vol. 2, no. 1, pp. 55–58, Mar. 2003.

[2] S. Li, Z. Yu, C. Rutherglen, and P. J. Burke, "Electrical properties of 0.4 cm long single walled carbon nanotubes," *Nano Lett.*, vol. 4, no. 10, pp. 2003–2007, 2004.

[3] S. Salahuddin, M. Lundstrom, and S. Datta, "Transport effects on signal propagation in quantum wires," *IEEE Trans. Electron Devices*, vol. 52, no. 8, pp. 1734–1742, Aug. 2005.

[4] J.-O. J. Wesström, "Signal propagation in electron waveguide: Transmission-line analogies," *Phys. Rev. B, Condens. Matter*, vol. 54, pp. 11484–11491, 1996.

[5] G. Miano, C. Forestiere, A. Maffucci, S. A. Maksimenko, and G. Ya. Slepyan, "Signal propagation in carbon nanotubes of arbitrary chirality," *IEEE Trans. Nanotechnol.*, 2010, to be published.

[6] Z. Yu and P. J. Burke, "Microwave transport in metallic single-walled carbon nanotubes," *Nano Lett.*, vol. 5, pp. 1403–1406, 2005.

[7] A. Naeemi and J. D. Meindl, "Impact of electron-phonon scattering on the performance of carbon nanotube interconnects for GSI," *IEEE Electron Device Lett.*, vol. 26, no. 7, pp. 476–478, Jul. 2005.

[8] A. Naeemi, R. Sarvari, and J. D. Meindl, "Performance comparison between carbon nanotube and copper interconnects for gigascale integration (GSI)," *IEEE Electron Device Lett.*, vol. 26, no. 2, pp. 84–86, Feb. 2005.

[9] A. Nieuwoudt and Y. Massoud, "Evaluating the impact of resistance in carbon nanotube bundles for VLSI interconnect using diameter-dependent modeling techniques," *IEEE Trans. Electron Devices*, vol. 53, no. 10, pp. 2460–2466, Oct. 2006.

[10] Y. Massoud and A. Nieuwoudt, "Modeling and design challenges and solutions for carbon nanotube-based interconnect in future high performance integrated circuits," *ACM J. Emerg. Technol. Comput. Syst.*, vol. 2, pp. 155–196, Jul. 2006.

[11] H. J. Li, W. G. Lu, J. J. Li, X. D. Bai, and C. Z. Gu, "Multichannel ballistic transport in multiwall carbon nanotubes," *Phys. Rev. Lett.*, vol. 95, pp. 086601: 1–086601: 4, 2005.

[12] A. Naeemi and J. D. Meindl, "Compact physical models for multiwall carbon-nanotube interconnects," *IEEE Electron Device Lett.*, vol. 27, no. 5, pp. 338–340, May 2006.

[13] D. Mencarelli, T. Rozzi, C. Camilloni, L. Maccari, A. Di Donato, and L. Pierantoni, "Modeling of multi-wall CNT devices by self-consistent analysis of multi-channel transport," *IOP Nanotechnol.*, vol. 19, Apr. 2008, Art. ID 165202, DOI: 10.1088/0957-4484/19/16/165202.

[14] D. Mencarelli, L. Pierantoni, and T. Rozzi, "Optical absorption of carbon nanotube diodes: Strength of the electronic transitions and sensitivity to the electric field polarization," *J. Appl. Phys.*, vol. 103, 2008, Art. ID 063103.

[15] L. Pierantoni, D. Mencarelli, and T. Rozzi, "Boundary immittance operator for the combined Schrödinger–Maxwell problem of carrier dynamics in nanodevices," *IEEE Trans. Microw. Theory Tech.*, vol. 57, no. 5, pp. 1147–1155, May 2009.

[16] G. Ya. Slepyan, S. A. Maksimenko, A. Lakhtakia, O. Yevtushenko, and A. V. Gusakov, "Electrodynamics of carbon nanotubes: Dynamic conductivity, impedance boundary conditions, and surface wave propagation," *Phys. Rev. B, Condens. Matter*, vol. 60, pp. 17136–17149, Dec. 1999.

[17] G. W. Hanson, "Drift diffusion: A model for teaching spatial dispersion concepts and the importance of screening in nanoscale structures," *IEEE Antennas Propag. Mag.*, Jan. 2010, submitted for publication.

[18] N. W. Ashcroft and N. D. Mermin, *Solid State Physics*. Philadelphia, PA: Holt, Rinehart, Winston, 1976.

[19] A. G. Chiariello, A. Maffucci, G. Miano, F. Villone, and W. Zamboni, "Metallic carbon nanotube interconnects, part II: A transmission line model," in *IEEE Signal Propag. Interconnects Workshop*, 2006, pp. 185–188.

[20] A. Maffucci, G. Miano, and F. Villone, "A transmission line model for metallic carbon nanotube interconnects," *Int. J. Circuit Theory Appl.*, vol. 36, pp. 31–51, 2006.

[21] W. Steinhögl, G. Schindler, G. Steinlesberger, M. Traving, and M. Engelhardt, "Comprehensive study of the resistivity of copper wires with lateral dimensions of 100 nm and smaller," *J. Appl. Phys.*, vol. 97, pp. 023706: 1–023706: 7, 2005.

[22] G. W. Hanson, "Radiation efficiency of nanoradius dipole antennas in the microwave and far-infrared regime," *IEEE Antennas Propag. Mag.*, vol. 50, pp. 66–77, Jun. 2008.

[23] S. M. Sze, *Semiconductor Devices*. New York: Wiley, 1985.

[24] M. Abramowitz and I. A. Stegun, *Handbook of Mathematical Functions*. Washington, DC: Nat. Bureau Standards, 1964.

[25] C. R. Paul, *Analysis of Multiconductor Transmission Lines*. New York: Wiley, 2007.

[26] S. Ilani, L. A. K. Donev, M. Kindermann, and P. L. McEuen, "Measurement of the quantum capacitance of interacting electrons in carbon nanotubes," *Nature Phys.*, vol. 2, pp. 687–691, 2006.

[27] G. Miano and F. Villone, "An integral formulation for the electrodynamics of metallic carbon nanotubes based on a fluid model," *IEEE Trans. Antennas Propag.*, vol. 54, pp. 2713–2724, Oct. 2006.

[28] D. M. Pozar, *Microwave Engineering*, 3rd ed. New York: Wiley, 2005.

[29] P. C. Clemmow and J. P. Dougherty, *Electrodynamics of Partcles and Plasmas*. Reading, MA: Addison-Wesley, 1969.

[30] R. Kragler and H. Thomas, "Dielectric function in the relaxation-time approximation generalized to electronic multiple-band systems," *Z. Phys. B, Condens. Matter*, vol. 39, pp. 99–107, 1980.

[31] A. R. Melnyk and M. J. Harrison, "Theory of optical excitation of plasmons in metals," *Phys. Rev. B, Condens. Matter*, vol. 2, pp. 835–850, Aug. 1970.

[32] N. D. Mermin, "Lindhard dielectric funstion in the relaxation-time approximation," *Phys. Rev. B, Condens. Matter*, vol. 1, pp. 2362–2363, Mar. 1970.

[33] P. Halevi, "Hydrodynamic model for the degenerate free-electron gas: Generalization to arbitrary frequencies," *Phys. Rev. B, Condens. Matter*, vol. 51, pp. 7497–7499, Mar. 1995.

[34] M. Dressel and G. Grüner, *Electrodynamics of Solids*. Cambridge, U.K.: Cambridge Univ. Press, 2002.

[35] L. Latessa, A. Pecchia, A. Di Carlo, and P. Lugli, "Negative quantum capacitance of gated carbon nanotubes," *Phys. Rev. B, Condens. Matter*, vol. 72, pp. 035455(1)–035455(5), 2005.

[36] A. Ishimaru, *Electromagnetic Wave Propagation, Radiation, and Scattering*. Englewood Cliffs, NJ: Prentice-Hall, 1991.

George W. Hanson (S'85–M'91–SM'98–F'09) was born in Glen Ridge, NJ, in 1963. He received the B.S.E.E. degree from Lehigh University, Bethlehem, PA, in 1986, the M.S.E.E. degree from Southern Methodist University, Dallas, TX, in 1988, and the Ph.D. degree from Michigan State University, East Lansing, in 1991.

From 1986 to 1988, he was a Development Engineer with General Dynamics, Fort Worth, TX, where he was involved with radar simulators. From 1988 to 1991 he was a Research and Teaching Assistant with the Department of Electrical Engineering, Michigan State University. He is currently Professor of electrical engineering and computer science at the University of Wisconsin–Milwaukee. He coauthored *Operator Theory for Electromagnetics: An Introduction* (Springer, 2002) and authored *Fundamentals of Nanoelectronics* (Prentice-Hall, 2007). His research interests include nanoelectromagnetics, mathematical methods in electromagnetics, electromagnetic wave phenomena in layered media, integrated transmission lines, waveguides, and antennas, and leaky wave phenomena.

Dr. Hanson is a member of URSI Commission B, Sigma Xi, and Eta Kappa Nu. He was an associate editor for the IEEE TRANSACTIONS ON ANTENNAS AND PROPAGATION from 2002 to 2007. He was the recipient of the 2006 S. A. Schelkunoff Best Paper Award of the IEEE Antennas and Propagation Society.